Proceedings of ASME TURBO EXPO 2007
Power for Land, Sea, and Air
May 14-17, 2007, Montreal, Canada

DRAFT GT2007-27993

Determination of Casing Convective Heat Transfer Coefficient and Reference Free-stream Temperature in the Tip Clearance Region of an Axial Flow Turbine

B. Gumusel[1] and C. Camci[2]

Turbomachinery Aero-Heat Transfer Laboratory
Department of Aerospace Engineering
The Pennsylvania State University
223 Hammond Building, University Park, PA 16802

ABSTRACT

The present study explains a steady-state method of measuring convective heat transfer coefficient on the casing of an axial flow turbine. The goal is to develop an accurate steady-state heat transfer method for the comparison of various casing surface and tip designs used for turbine performance improvements. The free-stream reference temperature, especially in the tip gap region of the casing varies monotonically from the rotor inlet to rotor exit due to work extraction in the stage. In a heat transfer problem of this nature, the definition of the free-stream temperature is not as straight forward as constant free-stream temperature type problems. The accurate determination of the convective heat transfer coefficient strongly depends on the magnitude of the local free-stream reference temperature varying in axial direction, from the rotor inlet to exit. The current study explains a strategy for the simultaneous determination of the steady-state heat transfer coefficient and free-stream reference temperature on the smooth casing of a single stage rotating turbine facility. The heat transfer approach is also applicable to patterned casing surfaces. A detailed uncertainty analysis follows a detailed description of the casing heat transfer measurements. The overall uncertainty of the method developed is between 5 % and 8 % of convective heat transfer coefficient.

1 Graduate Res. Assistant
2 Professor of Aerospace Engineering, corresponding author cxc11@psu.edu

INTRODUCTION

The convective heat transfer to the static casing of a shroudless HP turbine rotor is a complex aero-thermal problem. The unsteady flow with a relatively high Reynolds number in the tip gap region has strong dependency on the tip clearance gap, blade tip profile, blade tip loading conditions, blade tip geometry and casing surface character. Thermal transport by flow near the casing inner surface is influenced by the unsteadiness, the surface roughness character and the turbulent flow characteristics of the fluid entering into the region between the tip and casing. Since the turbine inlet temperatures are continuously elevated to higher levels, casing and tip related heat transfer issues are becoming more critical in design studies.

In gas turbines, the gas stream leaving the combustor is not at a uniform temperature in radial and circumferential directions. According to Butler et al [1] the combustor exit maximum temperature can easily be twice as high as the minimum temperature. The maximum temperature in general is around the mid-span and the lowest gas temperatures are near the walls. The mechanisms related to the distortion of the radial temperature profile as the combustor exit fluid passes through a turbine rotor are complex, as explained by Sharma and Stetson [2] and Harvey [3]. The hottest part of the fluid leaving the upstream nozzle guide vane tends to migrate to the rotor tip corner near the mid pressure surface of the blade. Unfortunately, mostly the hottest fluid originating from the mid span region of the combustor or NGV finds its way to the pressure side corner of the blade tip in the rotating frame. Details of hot streak migration in gas turbines can be found in Roback and Dring [4,5], Takanashi&Ni [6], Dorney et al. [7] and Dorney and Schwab [8].

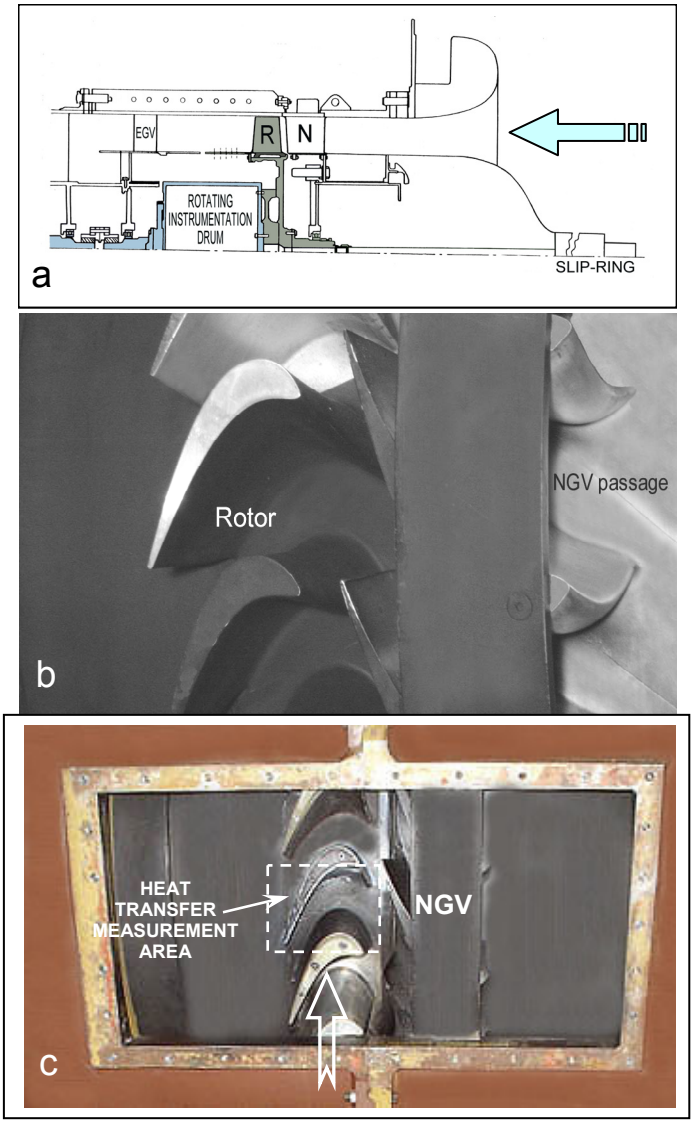

Figure 1 Axial Flow Turbine Research Facility (AFTRF)
a. facility schematic b. HP stage with 29 blades
c. window for removable casing segment

Due to significant energy extraction in a HP turbine stage, rotor absolute total temperature monotonically decreases in axial direction at a significant rate. This is especially true at the core of the blade passage where most of the energy extraction takes place. However, the fluid finding its way to the area between the casing and blade tips do not participate in the work generation as much as the mid-span fluid. Therefore, it is reasonable to accept that the near-casing fluid does not cool as much as the mid-span fluid when it progresses from rotor inlet to exit.

Yoshino [9] and Thorpe et al. [10] have shown that a rotor blade can also perform work on the fluid near the casing surface by means of "rotor compressive heating". They obtained time-accurate and phase-locked casing heat flux measurements in Oxford Rotor Facility to show the casing heat loads as the rotor blades move relative to the static casing. They observed a very high heat flux zone on the casing inner surface for each blade in the rotor. Phase-locked measurements clearly indicated that the hot spot moved along the casing with the rotor. The results of this study showed two distinct levels of casing heating, one level for the casing interaction with the tip leakage fluid and a relatively low level for the casing interaction with the passage fluid located between blade tips. Thorpe et al. [10] explained the high heat flux zone on the casing surface by a "rotor compressive heating" model. They showed that the static pressure field near the tip can do work on the leakage fluid trapped between the blade tip and the casing. The "rotor compressive heating" model predicts that the absolute total temperature of the leakage fluid may exceed that of the rotor inlet flow. The flow near the casing turns and accelerates the leakage fluid to a tangential velocity level that is measurably above the rotor inlet level. Thorpe et al. [11] were successful in predicting the total temperature penalty due to compressive heating using the Euler work equation. Any design effort that will reduce the tip leakage mass flow rate in an axial turbine will also result in the reduction of the total temperature penalty and a corresponding reduction in casing heat load.

Past studies show three significant contributors to casing heat loads in shroudless HP turbines.

1. Radially outward and axial migration of a hot streak in each passage results in the accumulation of relatively high temperature fluid near the pressure side corner of the blade tip before it enters the tip gap.

2. A relatively higher total temperature in the near-casing fluid is observed because the near casing fluid does not participate in stage work generation. The leakage fluid does not expand as much as the core-flow in the rotor passage.

3. Rotor compressive heating performed by blade tips when they move against the static casing is significant.

The near-casing gas temperature drops at a significant rate in axial direction. There is also a strong circumferential mixing near the casing because of the relative motion of blade tips. The time accurate wall heat flux measured on the casing vary between a "passage gas induced low value" and "tip leakage fluid induced high value". Since near-casing gas temperatures vary at a significant rate in axial direction, any heat transfer measurement approach requires the simultaneous measurement of this local gas temperature in the vicinity of the casing, in addition to an accurate determination of convective heat transfer coefficient. The present paper explains a steady-state method for the simultaneous determination of the casing heat transfer coefficient and the free-stream reference temperature using a smooth casing in a single stage rotating turbine facility. The heat transfer approach is also applicable to patterned casing surfaces. An uncertainty analysis follows a detailed description of the casing heat transfer measurements performed from a smooth casing surface.

EXPERIMENTAL SETUP & OPERATION

Turbine Research Facility: The facility used for the current casing heat transfer study, shown in Figure 1 is the Axial Flow Turbine Research Facility (AFTRF), at The Pennsylvania State University. A detailed description of the operational characteristics of this rotating rig is available in Camci [11]. The research facility is a large-scale, low speed, cold flow

turbine stage depicting many characteristics of modern high-pressure turbine stages. The total pressure and total temperature ratios across the stage are presented in Table 1 and air flow through the facility is generated by a four stage axial fan located downstream of the turbine. The rotor hub extends 1.7 blade tip axial chord length beyond the rotor exit plane. The turbine rig has a precision machined removable casing segment for measurement convenience especially for casing related aero-thermal studies. A few of the relevant design performance data are listed in Table 1, while Table 2 lists important blade design parameters, including reaction at blade hub and tip

Inlet Total Temperature : T_{o1} (K)	289
Inlet Total Pressure : P_{o1} (kPa)	101.36
Mass Flow Rate : Q (kg/sec)	11.05
Rotational Speed : N (rpm)	1300
Total Pressure Ratio : P_{o1}/P_{o3}	1.077
Total Temperature Ratio : T_{o3}/T_{o1}	0.981
Pressure Drop : P_{o1}-P_{o3} (mm Hg)	56.04
Power : P (kW)	60.6

Table 1 AFTRF Facility Design Performance Data

sections, Reynolds number at rotor exit and a few blade parameters. Measured/design values of rotor inlet flow conditions including radial, axial, tangential components and data acquisition details of the turbine rig are explained in detail by Camci [12] and Rao et al. [13].

Rotor hub-tip ratio	0.7269
Blade Tip Radius; R_{tip} (m)	0.4582
Blade Height; h (m)	0.1229
Relative Mach Number	0.24
Number of Blades	29
Axial Tip Chord; (m)	0.085
Spacing; (m)	0.1028
Turning Angle; Tip / Hub	95.42° / 125.69°
Nominal Tip Clearance; (mm)	0.9
Reaction, Hub / Tip	0.197 / 0.519
Reynolds Number (÷10^5) inlet / exit	(2.5~4.5) / (5~7)

Table 2 AFTRF Stage Blade & Vane Data

Instrumentation: Instruments used for monitoring the performance parameters of AFTRF consist of total pressure probes, Kiel probes, pitot-static probes, thermocouples, and a precision in-line torquemeter. The turbine rotational speed is kept constant around 1300 rpm by means of an Eddy current brake.

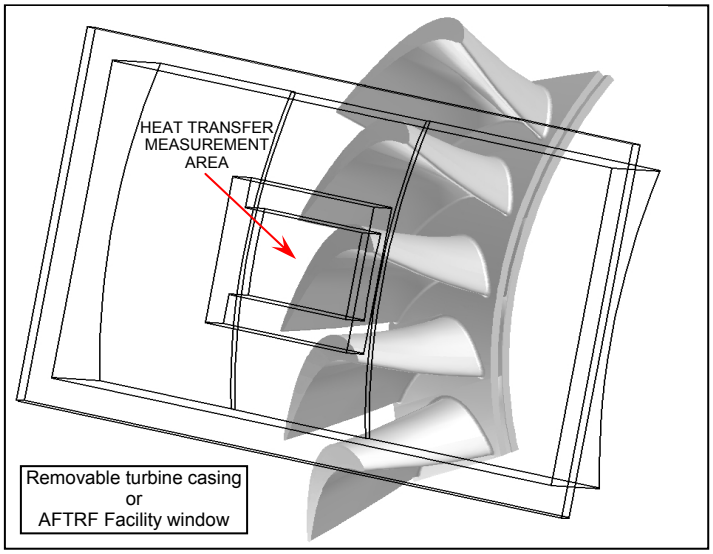

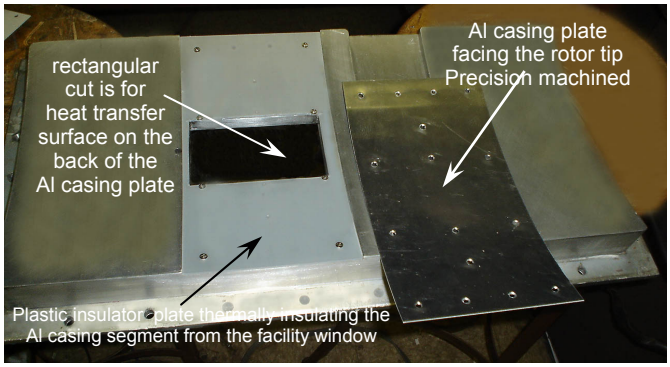

Figure 2 Removable turbine casing in (AFTRF)
(smooth partial "Al casing plate" is visible)

Removable Turbine Casing: Figure 1.c shows the facility window for the removable casing segment as a convenient feature of the test facility. A rectangular window that is six axial chord wide and four axial chord high is allocated for a removable casing segment. This segment is a precision machined area designed for many different areothermel measurement techniques to be applied around the turbine stage.

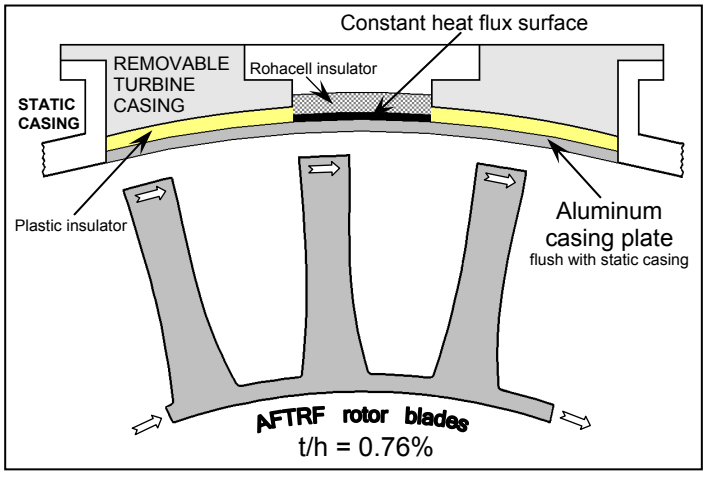

Figure 3 Removable turbine casing cross section
(normal to the axis of rotation)

Figure 2 shows the removable segment with the rectangular central area (dashed boundaries Figure 1.c) allowing the researchers to perform casing heat transfer measurements. The smooth Aluminum casing segment that is facing the rotor tip and interacting with near-casing fluid is also shown in detail in Figures 2 and 3. The Al casing plate could easily be replaced with custom made plates having casing treatments/patterns for tip vortex aerodynamic de-sensitization and supporting heat transfer studies. The removable turbine casing and the Al plate is carefully designed and precision machined so that many subsequent installations of the same Al plate and the removable window/casing result in a repeatable tip clearance. A tip clearance repeatability within ± 0.001 inch (25 micron) for a blade height of 4.85 inches (125 mm) is possible. This installation uncertainty corresponds to a change in non-dimensional tip clearance of 0.2 % of the blade height. Under normal circumstances, the inserted Al plate is supposed to be flush with the static casing of the facility. Slight clearance adjustments are possible for the removable segment by altering the thickness of the "plastic insulator" as shown in Figure 3. The baseline Al casing plate has the same radius of curvature as that of the casing. The average turbine tip clearance for the current experiments is kept at t/h=0.76 %.

Heat Transfer coefficient measurement locations: The five convective heat transfer coefficient measurement locations are shown in Figure 4. Location 1 is closest to the leading edge of the blade in axial direction. The five selected measurement locations cover the axial distance between the blade leading edge and slightly downstream of the trailing edge. Due to the rotation of the blade, the steady heat transfer coefficient distribution in circumferential direction is reasonably uniform. Since work is extracted in the rotor, the free-stream total temperature between the rotor inlet and rotor exit are different. Free-stream total temperature measurement locations at the turbine inlet, rotor inlet, rotor exit and turbine exit are also

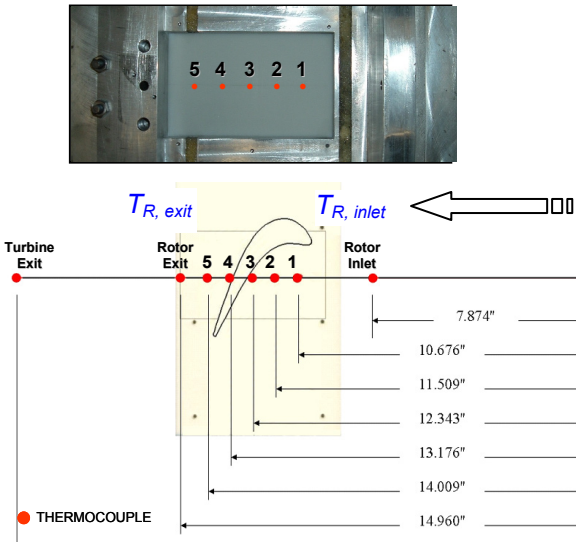

Figure 4 Heat Transfer coefficient measurement locations on the casing surface (five axial locations)

shown in Figure 4. The free-stream total temperatures at turbine inlet and exit are measured using calibrated K type thermo-

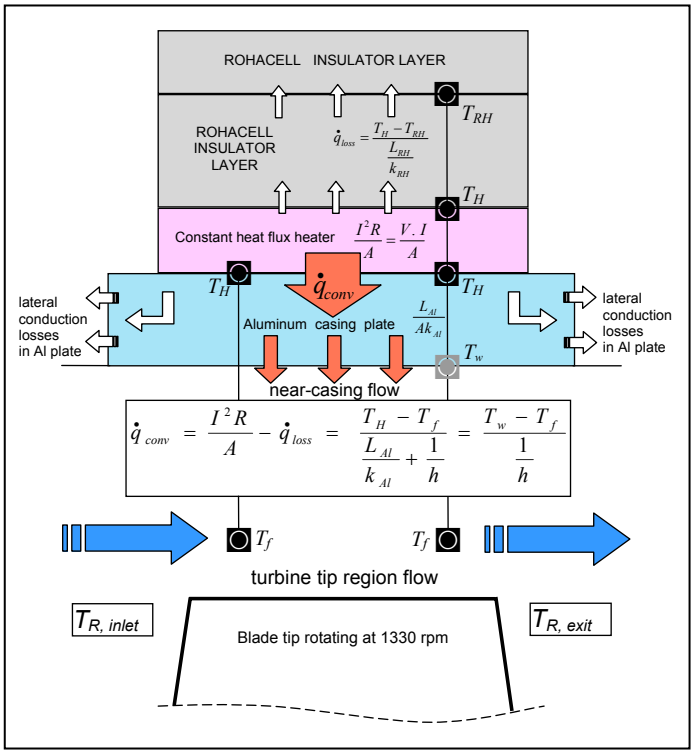

Figure 5 Heat Transfer model for convective heat transfer coefficient measurements on the turbine casing surface (the model allows for lateral conduction losses)

couples in a Kiel probe arrangement. Rotor inlet and exit thermocouples are fine wire K type thermocouples inserted into the flow at about 25 mm away from the casing surface.

Steady-state Heat Transfer Method: Casing convective heat transfer coefficients and corresponding fluid reference temperatures are measured simultaneously with the help of a constant heat flux heater as shown in Figure 5. A constant heat flux heater (MINCO Corp. *HK5175R176L12B*) with an effective area of (A=76x127 mm^2) is sandwiched between two thin Mylar sheets. The heater can produce max of 75 Watts with an overall resistance of 176 ohms. The current experiments do not exceed a power level of 12 Watts. The overall resistance of the 0.5 mm thick heater has extremely small temperature dependency in the range of the current experiments. This resistance value is continuously measured and recorded during each measurement. The Joule heating value in the heater is I^2R/A [Watts/m^2]. The heat transfer surface has many flat ribbon thermocouples of type K imbedded at many locations (symbol ◙ in Figure 5).

MATERIAL	Thermal Conductivity W/m-K	Thickness mm [inch]
ROHACELL	0.030	4.064 [0.160]
ALUMINUM PLATE	202.4	0.762 [0.030]
PLASTIC LAYER	0.120	1.397 [0.055]
HEATER (Minco)	0.981	0.500 [0.021]

Table 3 Thermal conductivity and thickness values for the heat transfer surface components

The thermocouple junctions are 12 μm thin. There are two thick layers of Rohacell insulating material flush mounted on top of the heater surface. Table 3 shows the material thicknesses in the heat transfer composite surface and thermal conductivity values. Current multi-dimensional heat conduction analysis shows that the lateral conduction of thermal energy at the edges of the heater surface and Rohacell insulator are extremely small and negligible. However the heat conduction loss $\dot{q}_{loss}$ in Rohacell in a direction normal to the heater is not negligible,

$$\dot{q}_{loss} = \frac{T_H - T_{RH}}{\frac{L_{RH}}{k_{RH}}} \quad . \qquad (1)$$

Due to extremely thin structure and the uniform internal heat generation by Joule heating in the volume of the heater, measured top and bottom surface temperatures ($T_{H)}$ are very close to each other . The amount of heat conducted through the Aluminum casing plate in a direction normal to the plate is,

$$\dot{q}_{conv} = \frac{I^2 R}{A} - \dot{q}_{loss} = \frac{T_H - T_f}{\frac{L_{Al}}{k_{Al}} + \frac{1}{h}} = \frac{T_w - T_f}{\frac{1}{h}} \quad . \quad (2)$$

Equation (2) shows the thermal energy per unit area per unit time crossing the fluid-solid interface between the near-casing turbine fluid and the Al casing plate when the lateral conduction losses in Al plate are ignored. Equation (2) also presents the convective heat transfer rate written between the heater T_H and the near-casing turbine fluid T_f. A heat transfer coefficient h can be measured in this approach without measuring the wall temperature T_w directly. In the present approach, h is first calculated from Equation (2) between T_H and T_f . The corresponding wall temperature T_w is then obtained from the last part of Equation (2) written between the wall and free stream,

$$T_w = T_H - (\dot{q}_{conv} \frac{L_{Al}}{k_{Al}}) \quad . \qquad (3)$$

A more accurate form of h can be obtained by quantifying lateral conduction losses in Aluminum plate. A three dimensional conduction heat transfer analysis including all three dimensional features of the removable turbine casing is presented in the next paragraphs. This computational effort reduces the measurement uncertainties in the local convective heat transfer coefficient h at a significant rate by calculating the lateral conduction losses on all four sides of the Al casing area that is face to face with the heater surface.

Lateral Conduction losses in Aluminum Casing Plate: Figure 6 presents results from a 3D heat conduction analysis for the removable turbine casing made up of solid Aluminum. The removable turbine casing is an extremely thick precision machined Aluminum with an average thickness of 50.8 mm (about 2 inches). The lateral heat conduction in the Aluminum casing plate in this experiment was deduced from this 3D heat conduction analysis performed under realistic thermal boundary conditions. The steady-state thermal conduction equation $\nabla^2 T(x,y,z) = 0$ was solved in the removable turbine casing with proper boundary conditions.

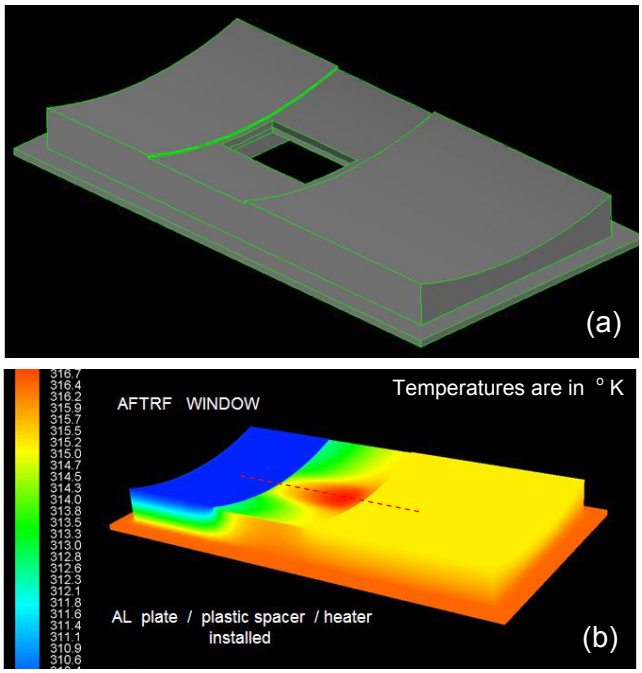

Figure 6 3D solid model and conduction analysis results on removable turbine casing surfaces

The constant heat flux heater shown in Figure5 is operated at a prescribed power I^2R [Watts] value. Joule heating in the heater was simulated by distributing this I^2R value uniformly over the volume of the thin heater as an internal heat generation u''' term. This is achieved by adding a source term to the energy equation in the numerical solution procedure. On the turbine

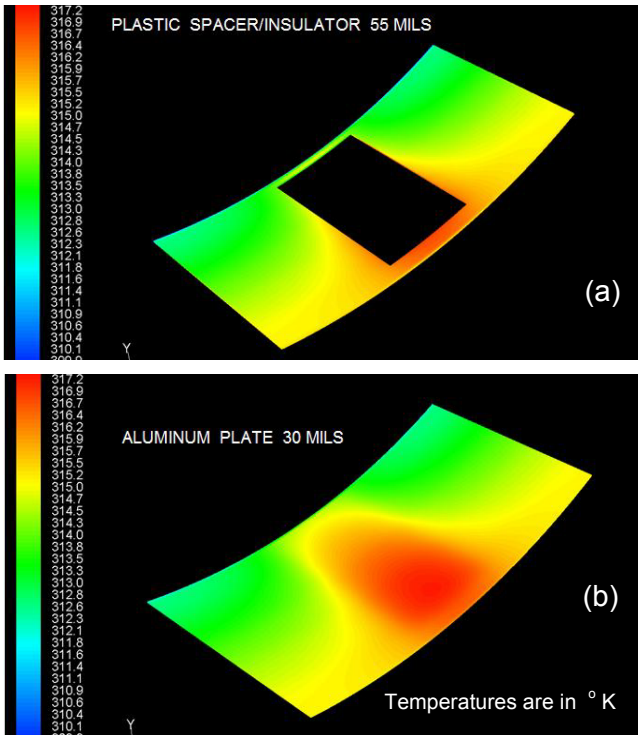

Figure 7 Temperature distributions on the plastic spacer and aluminum casing plate (flow side)

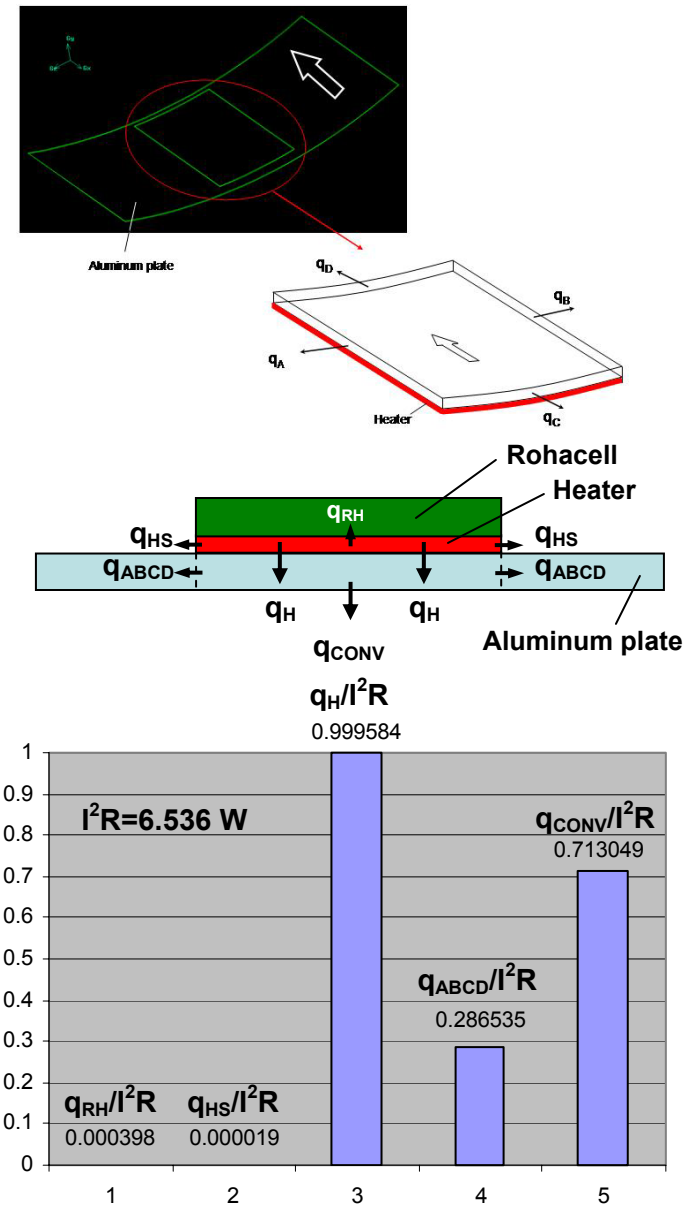

Figure 8 Casing plate lateral conduction from the four sides of the area facing the heater and the final energy balance

flow side, the surface temperature upstream of the rotor leading edge is taken as the measured turbine rotor inlet temperature (or NGV exit temperature). The flow side surface temperature downstream of the rotor trailing edge is the same as the measured rotor exit temperature. The flush mounted Aluminum casing plate has a convective type boundary condition on the flow side where a typical heat transfer coefficient h and a free-stream reference temperature is specified at five axial positions. Measured ambient temperature outside the rig is specified on the external flat face of the removable turbine casing. All other boundaries on the side walls were taken as adiabatic. The heater surface area is about the same as the small rectangular cut shown in figure 6.a. The temperature distribution on the Al casing plate facing the rotating blade tips is characterized by the red zone on top of the heater area. Along the red dashed line in the measurement area (in axial direction) the temperature distribution is reasonably uniform within half a degree K.

Figure 7.a shows the plastic spacer/insulator inserted between the removable turbine casing shown in Figure 6.a and the 0.030 inch thick casing plate shown in Figure 7.b. The heater is flush mounted on the convex side of the casing plate. Two layers of Rohacell were located on top of the heater surface in order to reduce heat losses to the ambient from the heater, Figure 5. The low conductivity plastic spacer is essential in this measurement approach in reducing the magnitude of the lateral conduction in the 0.030 ich thick casing plate. Figure 8 describes the lateral conduction heat losses from the Al casing plate. ($q_A+q_B+q_C+q_D$) is the sum of all thermal energy (in Watts) laterally conducted from the rectangular araea where the heater is flush mounted on the casing plate. q_{RH} is the heat loss through the Rohacell insulator and q_{HS} is the heat loss from the extremely narrow side faces of the heater volume with a thickness of 0.5 mm.

The bar chart prepared for the determination of lateral conduction heat loss as shown in Figure 8 is for $I^2R=6.536$ Watts. During the data reduction for h measurements, a new heat loss calculation was performed for each power setting using the 3D conduction solver with proper boundary conditions. Figure 8 shows that the heat loss through Rohacell layer and from the sides of the thin heater are extremely small when compared to the lateral conduction in the casing plate and the convective heat flux to the near-casing fluid. A proper correction of convection heat flux term $\dot{q}_{conv}$ in equation (2) for

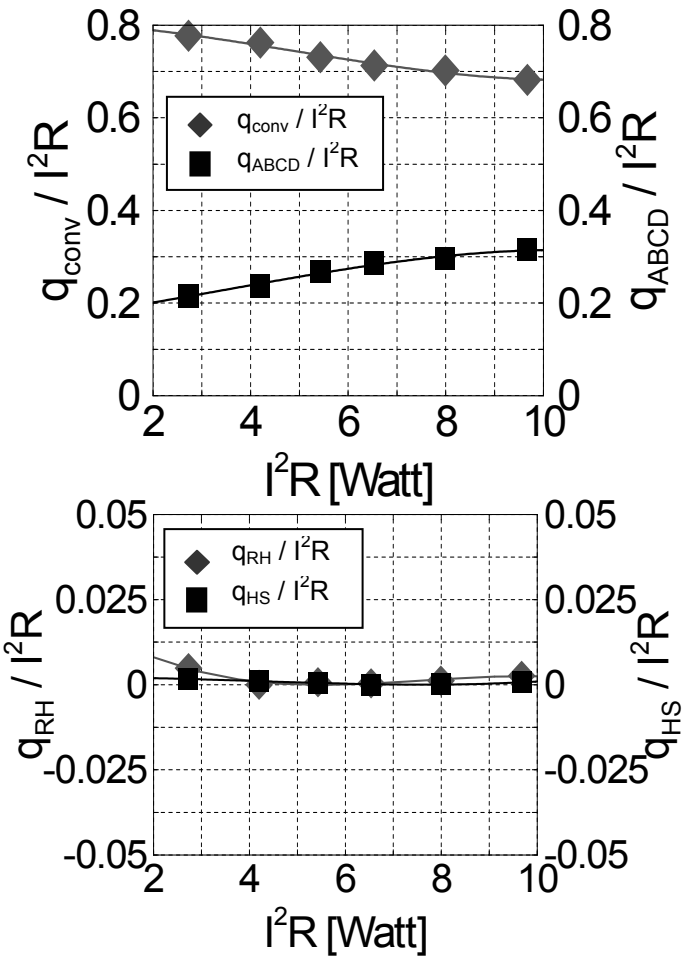

Figure 9 Energy balance in the heat transfer surface in function of power setting

lateral conduction losses is an important part of the overall data reduction process in obtaining heat transfer coefficients on the turbine casing surface. Figure 9 presents the variation of convective flux over area A $[\dot{q}_{conv} A]$, lateral conduction loss in casing plate, Rohacell layer losses and heater side losses in function of heater power setting I^2R .

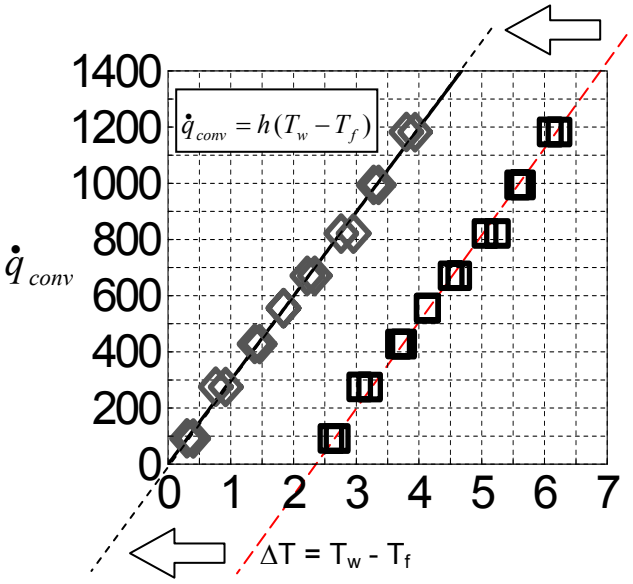

Figure 10 Simultaneous determination of convective heat transfer coefficient *h* and free stream reference temperature from multiple heater power settings

Heat Transfer Coefficient From Different Power settings: The convective heat transfer coefficient is measured by using an arranged form equation 2,

$$h = \frac{\dot{q}_{conv} k_{Al}}{k_{Al}(T_H - T_f) - L_{Al}\dot{q}_{conv}} \quad . \qquad (4)$$

$\dot{q}_{conv}$ can be obtained by substracting the heat losses from the Rohacell layer from $\frac{I^2R}{A} - \dot{q}_{loss}$ as shown in equation 2. T_H is measured from a thermocouple imbedded between the heater and the Al casing plate as shown in Figure 5. Finding the most accurate value of the reference fluid temperature T_f is crucial in this step. T_f is the reference free-stream fluid temperature in the vicinity of the casing surface facing the blade tips. Since this temperature monotonically decreases from rotor inlet to exit due to work extraction in the stage, an initial value is taken from the linear fit obtained from the measured turbine inlet $T_{R,inlet}$ and turbine exit $T_{R,exit}$ free-stream total temperatures , and as shown in Figure 5. The two measurement thermocouples for $T_{R,inlet}$ and $T_{R,exit}$ are inserted into the free-stream before and after the rotor. The junctions are in the turbine flow at about 1 inch away from the casing surface. The open square symbols in Figure 10 shows h measurements at axial location 1 obtained from many different heater power settings for the same turbine flow coefficient. The subsequent experiments are performed by gradually increasing the power setting to the heater. Maximum attention is paid to keep the corrected speed of the turbine facility constant. The dashed line fitted to square symbols in Figure 10 clearly shows that the wall heat flux $\dot{q}_{conv}$ versus $\Delta T=T_w-T_f$ is highly linear as expected in any forced convection heat transfer problem. Having multiple measurements of the same heat transfer coefficient h from many power settings makes an accurate measurement of the reference temperature T_f possible. According to the definition of the convective heat transfer coefficient h from $\dot{q}_{conv} = h(T_w - T_f)$, h is the slope of the linear relationship between convective heat flux and the temperature differental $\Delta T=T_w-T_f$. The long-dashed line in Figure 10 is also supposed to pass through origin because when $\dot{q}_{conv}$ is zero the wall is adiabatic and $T_f = T_w = T_{aw}$. This procedure corrects the value of initially "estimated" free-stream reference temperature T_f . This correction is only possible by establishing the long-dashed line from multiple h measurements at various power settings. If experimental procedure was perfect, two data points from only two power settings would establish the long-dashed line. The procedure described in this paragraph has the ability to measure the heat transfer coefficient h and free-stream reference temperature T_f simultaneously for this relatively complex measurement problem. The complexity in the measurement is in the fact that a direct measurement of T_f in the turbine in the tip gap region by a probe is extremely difficult. Another complexity is that the reference temperature continually drops in the turbine due to the work extraction process gradually building up in the in the axial direction.

Figure 10 is a good display of the fact that the measured heat transfer coefficient h (slope of the long-dashed line) is independently defined from the power setting and thermal boundary conditions $\Delta T=T_w-T_f$. Any suggested T_f can form a reasonably accurate h value that is the slope of the long dashed line. The long dashed line crosses ΔT axis at a specific value. When this value is added to the initially suggested T_f, , the correct free-stream reference temperature is obtained. The correct free-stream reference temperature for this problem is also called adiabatic wall temperature T_{aw} since it is the temperature of the wall occurring when the convective heat flux at the fluid solid interface is zero.

Axial Distribution of h on the casing plate: Figure 11 presents heat transfer coefficient data at all five axial locations defined in Figure 4. The same measurement methodology described in the previous paragraph is applied at all locations. A typical heat transfer experiment in AFTRF has an approximate duration of 50 minutes with h data from 8 to 10 power settings . It is recommended that no data is taken in the first 20 minutes to allow steady thermal and free-stream conditions to develop. The facility mass flow rate (flow coefficient) and stage total pressure drop (loading coefficient) are kept constant during this 50 minute run time by slightly changing the rotational speed of the rotor using a corrected speed definition. This approach helps to establish the dashed line in Figure 10 at a much better correlation coefficient.

Figure 12 shows the axial distribution oh h at five axial locations on the casing plate facing the blade tips.

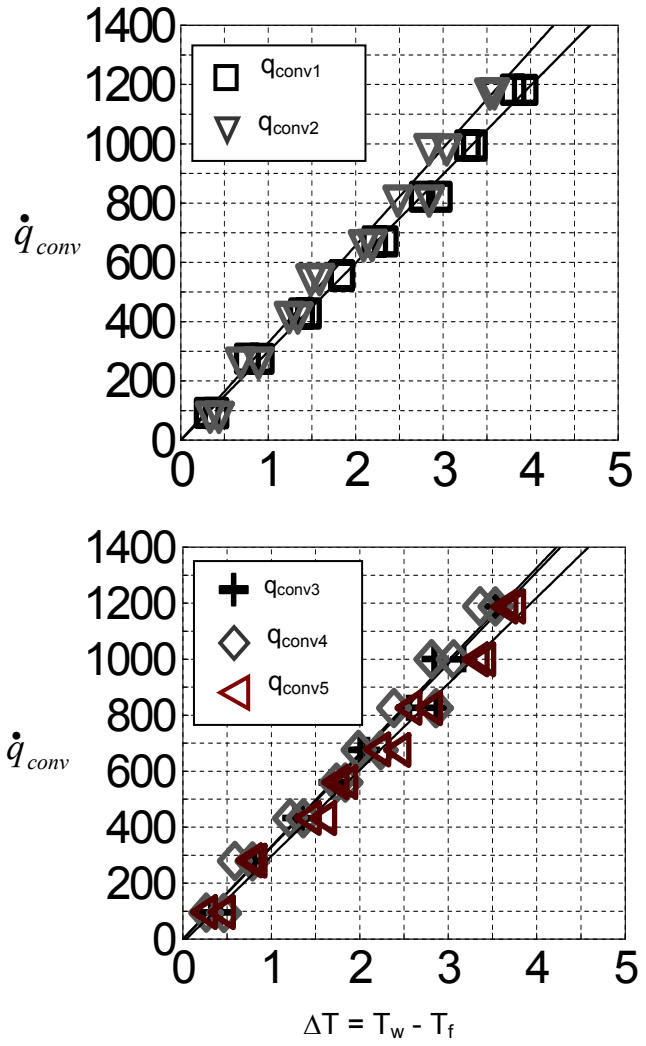

Figure 11 Heat transfer coefficient h at five axial locations on the casing plate surface facing the blade tips

The solid squares represent the data before a lateral conduction correction in the Aluminum casing plate is performed. The magnitude of lateral conduction losses are carefully determined from a 3D heat conduction analysis described in Figures 6 to 9. A proper heat loss analysis was performed for each power setting level carefully. A significant change in the overall magnitude of the heat transfer coefficients is observed after taking into account all energy losses from the Al casing plate, especially the lateral conduction losses. The measured h values do not show a strong axial position dependency. The casing plate measurement locations see the subsequent passage of tip leakage related fluid and passage fluid at blade passing frequency. The circumferential mixing in this near casing area is tremendous. A proper lateral conduction calculation is essential to reduce the experimental uncertainties in this heat transfer measurement approach.

Experimental Uncertainty Estimates : The most significant goal of this study was to establish a steady-state casing heat transfer measurement system with reduced uncertainties. Since

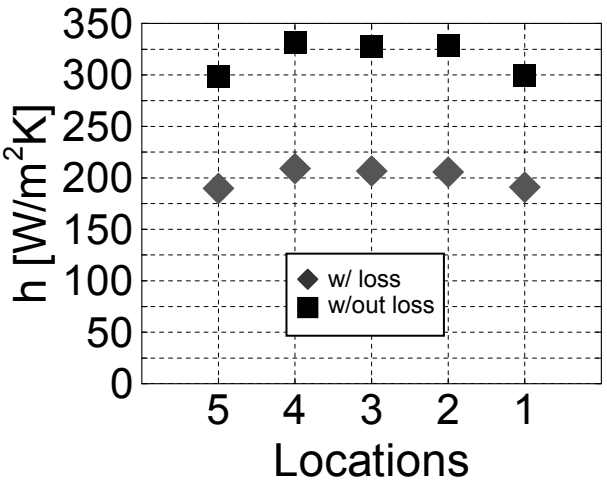

Figure 12 Distribution of the heat transfer coefficient with respect to axial position on the casing surface (without and with lateral conduction loss)

the number of parameters to be controlled in the rotating rig environment is much larger than a typical wind tunnel study, a detailed uncertainty analysis is essential to control and reduce the experimental errors. The specific uncertainty approach follows the concepts developed by Kline and McClintock [13]. Our uncertainty analysis is based on our basic measurement uncertainty estimates on reference free-stream temperature, heater surface temperature, thermal conductivity, plate thickness and Aluminum casing lateral conduction error.

QUANTITY	MEASUREMENT ERROR
T_f	$\delta T_f = \pm 0.15\ ^o K$
T_H	$\delta T_H = \pm 0.15\ ^o K$
k_{Al}	$\delta k_{Al} = \pm 0.222$ W/m-K
L_{Al}	$\delta L_{Al} = \pm 0.001$" (25 micron)
Lateral conduction error as a fraction of $\dot{q}_{conv}$	$\delta q/q = \pm 1\% - 5\%$
h	$\delta h/h = \pm 5\% - 8\%$

Table 4 Uncertainty estimates

Table 4 lists the magnitudes of all basic measurement uncertainties. Uncertainty analysis showed that very low heater power levels (less than 1 Watt) have a tendency to increase $\delta h/h$. The lateral conduction loss could vary from 1 % to 6 % even after numerically correcting for the lateral conduction. This uncertainty is introduced to account for edge heat flux variations around a mean $\dot{q}_{conv,}$ that already takes lateral conduction into account in a uniform way. The uncertainty of heat transfer coefficient is estimated to be in a range from 5 to 7 %.

CONCLUSIONS

A steady-state method for the measurement of convective heat transfer coefficient on the casing surface of an axial flow turbine is presented.

Special attention is paid to the static casing region facing the rotor blades. The current study shows that the uncertainty of the heat transfer coefficient h depends on the power setting level of the constant heat flux heater used in the measurement system.

A significant improvement for the uncertainty of h is possible by taking lateral conduction losses in the casing plate into account. The lateral conduction losses resulting from each power setting of the "constant heat flux heater" were numerically evaluated on a high resolution grid prepared for the removable casing model.

The current study presents a simultaneous measurement approach for both the heat transfer coefficient and the reference temperature of the near-casing fluid. The determination of the reference near-casing fluid temperature $T_f = T_{aw}$ from the current method is highly effective in reducing the heat transfer measurement uncertainty.

The method developed is very suitable for research turbine applications where the free stream fluid continuously cools from rotor inlet to rotor exit due to work extraction.

The present method is able to take the variation of many turbine run time parameters into account during a 50 minute run in which at least 10 heater power settings were used for the measurements.

A detailed uncertainty analysis is presented. The current heat transfer measurement method uncertainty is estimated to be between 5 % and 8% of convective heat transfer coefficient h.

The heat transfer evaluation of many casing surface modifications, patterns and blade tip shape modifications are possible with the specific method discussed in this paper.

ACKNOWLEDGMENTS

The authors acknowledge the valuable comments and advise provided by Dr. R.E.Chupp of GE Power Systems throughout this study. They are indebted to Mr.Harry Houtz, Rick Auhl , Mark Catalano, and Kirk Hellen for their outstanding technical support. The authors also acknowledge the valuable support from the Department of Aerospace Engineering at Penn State University.

NOMENCLATURE

h	convective heat transfer coefficient
h	also rotor blade height
I	DC current level to heater
I^2R	Joule heating in the heater *[W]*
k	thermal conductivity
L	material thickness
$Po1$	stage inlet total pressure, Pa
P_{o3}	stage exit total pressure, Pa
$\dot{q}_{conv}$	convective wall heat flux [W/m^2]
q_{conv}	convective heat flow through area A
q_{conv}	$[\dot{q}_{conv} A]$ *[W]*
q_{RH}	total heat flow through Rohacell insulator *[W]*
q_{ABCD}	lateral conduction loss in Al casing plate *[W]* (all four sides, see Figure 8)
q_{HS}	heat loss from the sides of the 0.5 mm thin heater *[W]*
r	radius
t	gap height between blade tip and outer casing, m
t/h	non-dimensional average clearance t/h=0.76 %
T_{aw}	adiabatic wall temperature
T_f	Free stream reference temperature *(T_{aw})*
$T_{R,inlet}$	rotor inlet free stream total temperature *(measured 1 25 mm away from casing)*
$T_{R,exit}$	rotor exit free stream total temperature *(measured 1 25 mm away from casing)*
U_m	rotor blade speed at mid-height location
V	velocity
V	also DV voltage applied to heater
θ,x,r	tangential, axial, radial components

subscripts

aw	adiabatic wall
Al	Aluminum
f	free stream fluid reference
H	heater
RH	Rohacell insulator material
w	wall

REFERENCES

1. Butler, T.L., Sharma O.P., Joslyn, H.T., Dring, R.P., 1989 "Redistribution of an inlet Temperature Distribution in an Axial Flow Turbine Stage," AIAA Journal of Propulsion, .Vol.5, No.1, pp.64-71.

2. Sharma, O.P., Stetson, G.M., 1998, "Impact of Combustor Generated Temperature Distortions on Performance, Durability and Structural Integrity of Turbines," VKI Lecture Series 1998-02, Feb.9-12, Brussels, Belgium.

3. Roback, R.J., Dring, R.P., 1992, “Hot Streaks and Phantom Cooling in a Turbine Rotor Passage, *Part-1 Separate Effects*,” ASME paper 92-GT-75.

4. Roback, R.J., Dring, R.P., 1992, “Hot Streaks and Phantom Cooling in a Turbine Rotor Passage, *Part-2 Combined Effects and Analytical Modelling*,” ASME paper 92-GT-76.

5. Takanishi, R.K., Ni, R.H., 1990, ”Unsteady Euler Analysis of the Redistribution of an Inlet Temperature Distortion in a Turbine, AIAA paper 90-2262.

6. Dorney, D.J., Davis, R.L., Edwards, D.E., Madavan, N.K., 1990, “Unsteady Analysis of Hot Streak Migration in a Turbine Stage, AIAA-90-2354.

7. Dorney, D.J. and Schwab, R.J., 1995, “Unsteady Numerical Simulations of Radial Temperature Profile Redistribution in a Single Stage Turbine,” ASME paper 95-GT-178.

8. Yoshino, S., 2002, “Heat Transfer in Rotating Turbine Experiments,” D.Phil. Thesis, Oxford University.

9. Thorpe, S.J.,Yoshino, S., Ainsworth, R.W., Harvey, N.W., 2004, “An Investigation of the Heat Transfer and Static Pressure on the Over-tip Casing Wall of an Axial Turbine Operating at Engine Representative Flow Conditions: *Part I, Time-mean Results,"* International Journal of Heat and Fluid Flow.

10. Thorpe, S.J, Yoshino, S, Ainsworth, R.W., Harvey, N.W., 2004, “An Investigation of the Heat Transfer and Static Pressure on the Over-tip Casing Wall of an Axial Turbine Operating at Engine Representative Flow Conditions: *Part I, Time-resolved Results*," International Journal of Heat and Fluid Flow.

11. Camci, C., 2004, Experimental and Computational Methodology for Turbine Tip De-sensitization. *VKI Lecture Series 2004-02*, “Turbine Blade Tip Design and Tip Clearance Treatment,” 2004.

12. Rao, M.N., Gumusel, B., Kavurmacioglu, L., and Camci, C., 2006, “Influence of Casing Roughness on the Aerodynamic Structure of Tip Vortices in an Axial Flow Turbine,” ASME paper GT 2006-91011.

13. Kline, S.J., McClintock, F.A., 1953, “Describing Uncertainties in Single-Sample Experiments.” Mechanical Engineering, Vol.75, pp.3- 11.

Appendix-A

Uncertainty Analysis

Influence of power setting (I^2R level), reference temperature measurement error δT_f, Lateral conduction error $\delta q/q$
on
convective heat transfer coefficient measurement error $\delta h/h$

$$h = \frac{\dot{q}_{conv} k_{Al}}{k_{Al}(T_H - T_f) - L_{Al}\dot{q}_{conv}}$$

$\frac{\delta q}{q}$ ⇒ Error in the specification of $\dot{q}_{conv}$ in equations 2&3

$$\delta h = \left[\left(\frac{\partial h}{\partial q}\delta q\right)^2 + \left(\frac{\partial h}{\partial k}\delta k\right)^2 + \left(\frac{\partial h}{\partial T_H}\delta T_H\right)^2 + \left(\frac{\partial h}{\partial T_f}\delta T_f\right)^2 + \left(\frac{\partial h}{\partial L}\delta L\right)^2 \right]^{1/2}$$

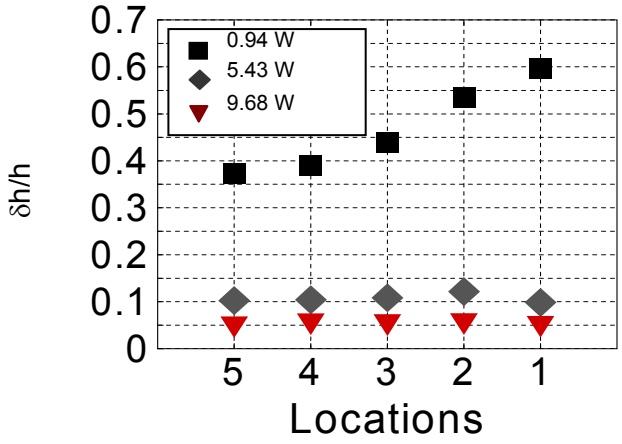

$\delta T_f = \pm 0.1$ °K , $\delta T_H = \pm 0.15$ °K , $\delta q/q = \pm 0.01$, $\delta k = \pm 0.196$ W/mK , $\delta L = \pm 1$ mils

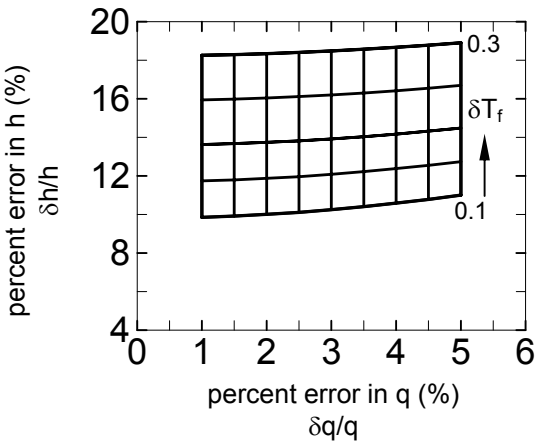

$I^2R = 5.43$ W , $\delta T_f = \pm 0.1 \div 0.3$ °K
$\delta T_H = \pm 0.15$ °K, $\delta k = \pm .0196$ W/mK, $\delta L = \pm 1$ mils

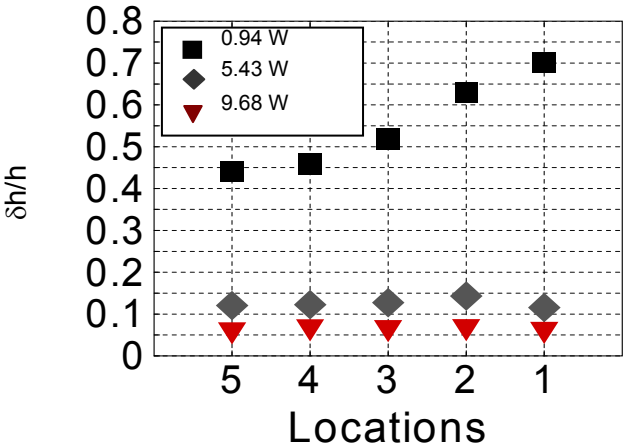

$\delta T_f = \pm 0.15$ °K , $\delta T_h = \pm 0.15$ °K , $\delta q/q = \pm 0.01$, $\delta k = \pm 0.196$ W/mK , $\delta L = \pm 1$ mils

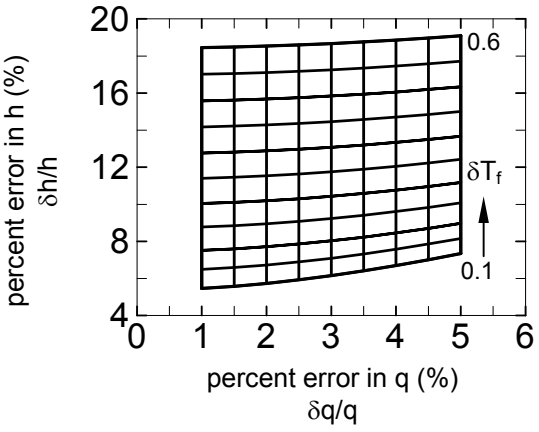

$I^2R = 9.68$ W , $\delta T_f = \pm 0.1 \div 0.6$ °K
$\delta T_h = \pm 0.15$ °K , $\delta k = \pm 0.196$ W/mK, $\delta L = \pm 1$ mils